Regulatory implications of a novel mode of interaction of calmodulin with a double IQ-motif target sequence from murine *dilute* myosin V

STEPHEN R. MARTIN AND PETER M. BAYLEY

Division of Physical Biochemistry, National Institute for Medical Research, Mill Hill, London NW7 1AA, UK

(RECEIVED April 11, 2002; FINAL REVISION July 17, 2002; ACCEPTED September 4, 2002)

Abstract

Apo-Calmodulin acts as the light chain for unconventional myosin V, and treatment with Ca^{2+} can cause dissociation of calmodulin from the 6IQ region of the myosin heavy chain. The effects of Ca^{2+} on the stoichiometry and affinity of interactions of calmodulin and its two domains with two myosin-V peptides (IQ3 and IQ4) have therefore been quantified in vitro, using fluorescence and near- and far-UV CD. The results with separate domains show their differential affinity in interactions with the IQ motif, with the apo-N domain interacting surprisingly weakly. Contrary to expectations, the effect of Ca^{2+} on the interactions of either peptide with either isolated domain is to increase affinity, reducing the K_d at physiological ionic strengths by >200-fold to ~75 nM for the N domain, and ~10-fold to ~15 nM for the C domain. Under suitable conditions, intact (holo- or apo-) calmodulin can bind up to two IQ-target sequences. Interactions of apo- and holo-calmodulin with the double-length, concatenated sequence (IQ34) can result in complex stoichiometries. Strikingly, holo-calmodulin forms a high-affinity 1:1 complex with IQ34 in a novel mode of interaction, as a "bridged" structure wherein two calmodulin domains interact with adjacent IQ motifs. This apparently imposes a steric requirement for the α-helical target sequence to be discontinuous, possibly in the central region, and a model structure is illustrated. Such a mode of interaction could account for the Ca^{2+}-dependent regulation of myosin V in vitro motility, by changing the structure of the regulatory complex, and paradoxically causing calmodulin dissociation through a change in stoichiometry, rather than a Ca^{2+}-dependent reduction in affinity.

Keywords: Calmodulin; IQ motif; myosin V; motility; regulatory complex

Calmodulin is primarily known as the highly conserved, ubiquitous intracellular receptor for calcium signals in eukaryotic cells, which promotes Ca^{2+}-dependent regulation of numerous biological processes (Berridge et al. 2001; Chin and Means 2001). The holo-CaM complex activates a wide variety of target enzymes, including kinases and kinase cascades (Soderling 1999). Conformational changes occurring in both calmodulin domains when each binds two calcium ions (Finn et al. 1995; Kuboniwa et al. 1995; Zhang et al. 1995) expose hydrophobic surfaces with which key hydrophobic residues of a given target sequence interact (Crivici and Ikura 1995; Rhoads and Friedberg 1997). Enzyme activation typically occurs by removal of a contiguous or noncontiguous inhibitory pseudosubstrate sequence of the enzyme from its own active site (Kemp et al. 1987).

Information on the molecular interaction of Ca_4CaM with target enzymes depends mainly on structures of complexes of calmodulin with synthetic peptides of ~20 residues in length, often with a basic, amphipathic, α-helical motif, representing the calmodulin target sequence of numerous kinases. This type of target interaction has been extensively analyzed in terms of the structural changes on binding to

Reprint requests to: Peter M. Bayley, Division of Physical Biochemistry, National Institute for Medical Research, Mill Hill, London NW7 1AA, UK; e-mail: pbayley@nimr.mrc.ac.uk; fax: 44-208-906-4477.

Abbreviations: IQ3, Ac-AATTIQKYWRMYVVRRRYK-NH_2; IQ4, Ac-IRRAATIVIQSYLRGYLTRNRYR-NH_2; IQ34, Ac-AATTIQKYWRMYVVRRRYKIRRAATIVIQSYLRGYLTRNRYR-NH_2; CaM, calmodulin; apo-CaM, Ca^{2+}-free calmodulin; holo-CaM, Ca_4CaM, Ca-saturated calmodulin; Tr1C, tryptic fragment 1: calmodulin N domain, residues 1–77; Tr2C, tryptic fragment 2: calmodulin C domain, residues 78–148.

Article and publication are at http://www.proteinscience.org/cgi/doi/10.1110/ps.0210402.

calmodulin (Finn et al. 1995; Kuboniwa et al. 1995; Zhang et al. 1995), the sequence requirements of the target protein (Crivici and Ikura 1995; Rhoads and Friedberg 1997), the relative affinities of individual domains of calmodulin for given sequences (Bayley et al. 1996), the ability of individual domains to activate certain enzymes (Persechini et al. 1994), and the discrimination between domains effected by the competition of Ca^{2+} and Mg^{2+} ions under physiological conditions (Martin et al. 2000).

The resulting picture is that calmodulin exhibits an almost unique versatility for its Ca^{2+}-dependent interactions with targets, governed by (1) the differential affinity of the two domains for Ca^{2+} (Linse et al. 1991) and for Mg^{2+} (Martin et al. 2000); (2) the differential affinity of the two (Ca^{2+}-loaded) domains for given target sequences (Barth et al. 1998), portions of which are normally, but not necessarily, contiguous; (3) the resulting structures of Ca_4CaM complexes differing in terms of the relative disposition of the two domains relative to the (generally) α-helical target sequence (Meador et al. 1993); and (4) the possibility of differences in orientation of the target peptide relative to one or more of the domains of calmodulin (Barth et al. 1998; Osawa et al. 1999; Kurokawa et al. 2001). The recent structure of the complex of calmodulin with the gating domain of the Ca^{2+}-activated K^+ channel (Schumacher et al. 2001), interactions of calmodulin with several L-types of Ca^{2+} channels (Erickson et al. 2001), and the structure of the anthrax adenylyl cyclase exotoxin (Drum et al. 2002) are further examples of the molecular versatility of calmodulin in its target reactions.

The interaction of apo-CaM with target sequences has been less studied. Its affinity for the kinase-type target sequences is typically many orders of magnitude lower than Ca_4CaM (Tsvetkov et al. 1999; Martin et al. 2000). In contrast, both apo-CaM and Ca_4CaM bind to the neuronal protein neuromodulin (GAP-43 or P-57) with similar affinity (Cimler et al. 1985; Alexander et al. 1987). This protein contains a different type of CaM target sequence, the IQ motif, with consensus sequence IQxxxRGxxxR. This motif is found as a single copy in other neuronal proteins, such as neurogranin (RC3) and PEP19, and also occurs, typically in multiple concatenated forms, in the large family of cytoplasmic myosin motor proteins (Cheney and Mooseker 1992). In these unconventional myosins, calmodulin acts as a "light chain," analogous to the two specific light chains (essential and regulatory light chains, ELC and RLC) of the (conventional) myosin II (Cope et al. 1996; Houdusse et al. 1996). The ELC and RLC binding sequences are also IQ motifs, but they diverge in part from the consensus sequence observed in the unconventional myosins (Houdusse et al. 1996).

Present models of myosin motor protein mechanisms are based on the crystal structures of muscle myosin II, in which the α-helical IQ sequences (plus ELC and RLC) constitute the "lever arm" regulatory region involved in the mechanico-chemical coupling between the ATPase site (in the globular S1 head) and the C-terminal coiled-coil dimerization structures (Houdusse et al. 1999). The length of the IQ region has been shown to correlate with motor speed and step size in the in vitro motility assays with (conventional) myosin II (Anson et al. 1996; Uyeda et al. 1996; Ruff et al. 2001). But recent evidence makes us question whether this relationship also holds for other members of the myosin family, such as myosin V and VI (for review, see Geeves 2002).

The molecular basis of IQ–calmodulin interactions is critical for understanding the activity and regulation of these unconventional myosin motor proteins. A model of the structure of apo-CaM complexed with the IQ1 sequence of the unconventional myosin, brush border myosin-I, BBM1 (1aji.pdb; Houdusse et al. 1996) was derived from the ELC portion of the atomic structure of the regulatory fragment of scallop myosin II (1wdc.pdb), showing the ELC and the RLC bound to residues 781–837 of the α-helical myosin heavy chain (Houdusse and Cohen 1996). The structure of apo-CaM with the IQ12 peptide sequence of myosin V has also been reported (Houdusse et al. 2000). These models indicate that both domains of apo-CaM interact with different parts of the IQ motif, and in distinctly different modes, with the C domain in the semiopen conformation, and the N domain in the closed conformation (Houdusse et al. 1996; Swindells and Ikura 1996).

Regulation of unconventional myosins I and V by Ca^{2+} has been shown in an in vitro motility assay, based on the ATP-dependent movement of fluorescent actin filaments on the S1 subfragment of the myosin attached to a surface. The motility was inhibited by $[Ca^{2+}] \sim 100$ μM (pCa ~4), and was restored only by the inclusion of apo-CaM together with EGTA. The proposal that Ca^{2+} causes the dissociation of CaM from the IQ regions has been supported by gel analysis for both myosin I (Collins et al. 1990; Zhu et al. 1998) and myosin V (Zhu et al. 1996). However, the motility of both myosin I and myosin V can be inhibited at significantly lower $[Ca^{2+}]$ (pCa ~6) without apparently causing calmodulin dissociation (Zhu et al. 1998; Homma et al. 2000).

The aim of the present work is to characterize the effect of Ca^{2+} on the interaction of calmodulin (and its separate constituent domains) with well-conserved peptide sequences derived from portions of the IQ region of mouse *dilute* myosin V. Here we study peptides IQ3, IQ4, and the double-length sequence IQ34. Near-UV and far-UV CD and fluorescence spectroscopy are used to assess quantitatively the stoichiometry and affinity of complex formation, in both the presence and absence of Ca^{2+}. These interactions are shown to be strikingly different from those of Ca_4CaM with basic, α-helical target peptides, in which Ca^{2+} typically increases target affinity by up to 10^6-fold (Bayley et al. 1996).

Under physiological ionic conditions, both Ca_4CaM and apo-CaM can interact with a given IQ sequence with high affinity ($K_d < 100$ nM), and the presence of Ca^{2+} surprisingly enhances the affinity of calmodulin for a given peptide. Ca_4CaM can bind up to two IQ-target sequences, one to each domain. There is a strong differential effect of the two domains of apo-CaM, with the C domain accounting for the majority of the affinity of complex formation. The interactions of apo-CaM (and its domains) with IQ peptides are strongly ionic strength-dependent, and multiple stoichiometry can result. The behavior becomes even more complex with the concatenated, double-length IQ motif IQ34, which forms a novel 1:1 complex with Ca_4CaM. These results are discussed with reference to the possible molecular mechanism of the inhibitory effect of Ca^{2+} on the motility of unconventional myosins.

Results

Because *Drosophila* calmodulin contains no tryptophan residues, the single Trp residue in the IQ3 peptide was used for direct monitoring of complex formation with calmodulin or its separate domains using Trp fluorescence emission and near-UV CD. These optical properties were also used in titrations in which IQ4 was used to displace IQ3 from complexes with calmodulin or its domains.

Interaction of IQ3 and IQ4 with the calmodulin fragments

Figure 1A shows the Trp fluorescence emission spectra for the complexes of IQ3 with the calmodulin fragments, Tr1C and Tr2C. The emission maxima are at 338 (apo-Tr1C), 335 (holo-Tr1C), 334 (apo-Tr2C), and 328 nm (holo-Tr2C). The free peptide emits at ~356 nm. These spectra show that both fragments form complexes in which they interact with the Trp-containing portion of the peptide. In both cases the solvent exposure of the Trp residue is further decreased in the complex with the Ca^{2+}-saturated fragment.

Fluorescence titrations of IQ3 with the calmodulin fragments are shown in Figure 1B. Apo-Tr1C was found to interact weakly with IQ3 at physiological ionic strength (see below), and this titration was therefore performed at low KCl concentration (10 mM). These titrations show that the apo- and holo-forms of the fragments form simple 1:1 complexes with the IQ3 peptide. There is no evidence that this peptide binds a second copy of the fragment under the concentration conditions of these experiments.

Preliminary studies using far-UV CD showed that IQ3 (and IQ4) became partially helical when bound to the calmodulin fragments, both with and without Ca^{2+}. Titrations of the fragments with IQ3 show that 1:1 complexes are formed in each case (Fig. 2A). In the case of Tr1C, the increase in helicity is very similar in the apo and holo cases.

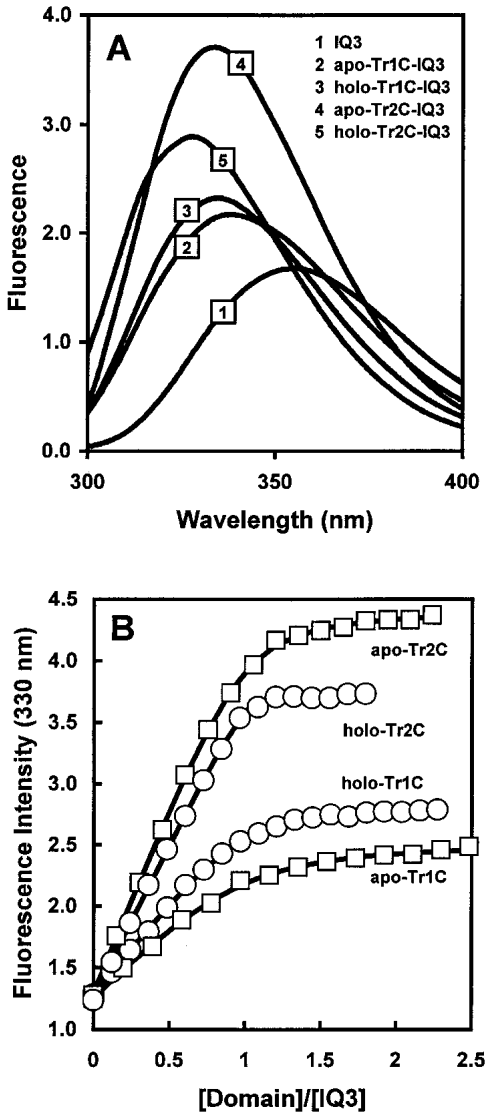

Fig. 1. (*A*) Fluorescence emission spectra of IQ3 and its complexes with apo-Tr1C, holo-Tr1C, apo-Tr2C, and holo-Tr2C. Spectra were recorded in 25 mM Tris, 10 mM KCl (pH 8.0) with 0.2 EGTA or 1 mM $CaCl_2$ as appropriate. (*B*) Fluorescence titrations of IQ3 (2.55 μM) with apo-Tr1C (K_d = 270 nM), holo-Tr1C (K_d = 98 nM), apo-Tr2C (K_d = 85 nM), and holo-Tr2C (K_d = 11 nM). Titrations were performed at 20°C in 25 mM Tris (pH 8.0) with 10 mM KCl (apo-Tr1C) or 100 mM KCl (apo- and holo-Tr2C, holo-Tr1C). Solutions contained 0.2 mM EGTA or 1 mM $CaCl_2$ as appropriate. Solid lines are the computed best fits for 1:1 stoichiometry, with the K_d values as indicated.

The increase in helicity is significantly greater for IQ3 bound to Tr2C compared with Tr1C (for both the apo and holo cases), and, surprisingly, this increase is larger for the complex with apo-Tr2C than for the complex with holo-Tr2C. Similar far-UV CD titrations performed with IQ4 (Fig. 2B) show that this peptide gives similar increases in CD intensity upon forming 1:1 complexes with the fragments. IQ4, like IQ3, becomes more helical in complexes

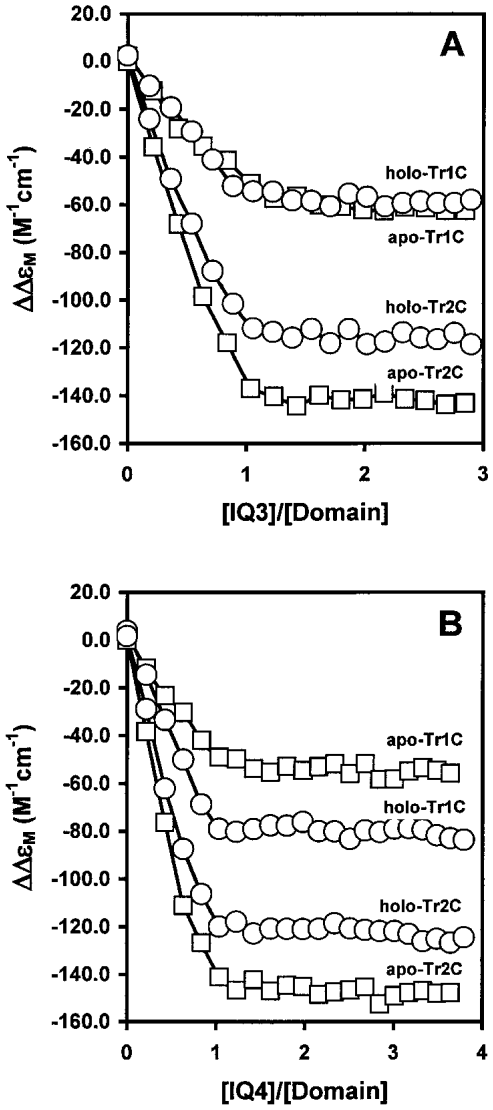

Fig. 2. Far-UV CD titrations (222 nm) of the calmodulin fragments with IQ3 (*A*) and IQ4 (*B*). Titrations were performed using 10–12 μM protein at 20°C in 25 mM Tris (pH 8.0), 10 mM KCl with 0.2 mM EGTA or 1 mM $CaCl_2$ as appropriate. The signal plotted was calculated as $\Delta\Delta\varepsilon_M = (\Delta A_{Observed} - \Delta A_{Domain} - \Delta A_{Peptide})/[Domain]$, where $\Delta A_{Observed}$ is the signal observed during the titration, ΔA_{Domain} is the signal from the domain alone, and $\Delta A_{Peptide}$ is the signal from the peptide alone. [Domain] is the molar concentration of the domain.

with Tr2C than in those with Tr1C, and is more helical in the complex with apo-Tr2C than in the complex with holo-Tr2C. With Tr1C, the situation is reversed, IQ4 being more helical in the complex with the holo-form than with the apo-form. These results show the general effect that either peptide will bind to either domain in the presence or absence of Ca^{2+}, with a corresponding increase in overall helicity. The results indicate a domain and peptide specificity in the resulting intensities of all the 1:1 peptide–fragment complexes, indicating significant differences in secondary structure, with the greater effects shown by both peptides in complex with the C domain.

Because both peptides form 1:1 complexes with the calmodulin fragments, fluorescence competition assays were used to measure affinities for the complexes involving IQ4 (which is spectroscopically silent). In these experiments (Fig. 3) a mixture of IQ3 and excess fragment was titrated with IQ4, and the decrease in Trp fluorescence was monitored. (The titration involving apo-Tr1C was again performed at low ionic strength; see above.) The curves were analyzed using the values of the affinities for IQ3 determined using the direct titrations (Fig. 1B). Dissociation constants for IQ4 binding to apo- and holo-Tr2C are approximately twofold higher than those for the binding of IQ3. The differences are significantly greater for Tr1C; the K_d for the binding of IQ4 to apo-Tr1C is fivefold higher than that for IQ3, but the K_d for binding to holo-Tr1C is threefold lower. To confirm that the competition assay provides a reliable estimate for the K_d of IQ4, a far-UV CD titration of apo-Tr2C with IQ4 was performed, at an ionic strength of 220 mM. Analysis of this curve (data not shown) gave a K_d of 1.4 ±0.6 μM, in reasonable agreement with the value determined using the competition assay (see Table 1).

A combination of direct fluorometric and fluorescence competition titrations was used to measure the affinity for the interaction of IQ3 or IQ4 with the calmodulin fragments over a range of ionic strengths. The results are summarized in Figure 4 and Table 1. These data clearly illustrate the greater ionic-strength dependence in the formation of the complexes of IQ3 (or IQ4) with the apo-form of Tr1C or Tr2C, compared with the holo-complexes. The weakness of

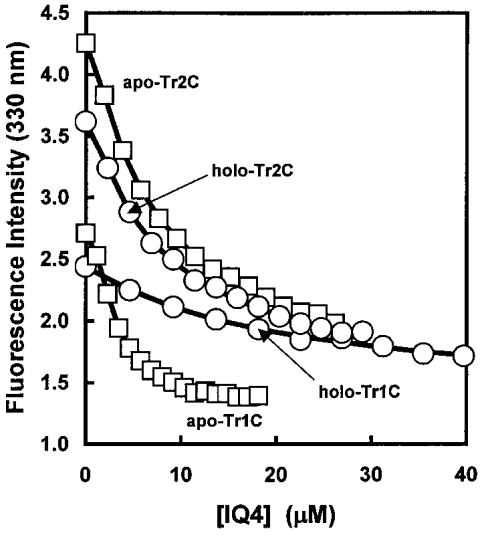

Fig. 3. Fluorescence competition titrations of IQ3 (2.55 μM) plus excess calmodulin domain (3.65–4.0 μM) with IQ4. Titrations were performed at 20°C in 25 mM Tris (pH 8.0) with 10 mM KCl (apo-Tr1C) or 100 mM KCl (apo- and holo-Tr2C, holo-Tr1C). Solutions also contained 0.2 mM EGTA or 1 mM $CaCl_2$ as appropriate. The solid lines are the computed best fits.

Table 1. *Dissociation constants for the interaction of IQ3 and IQ4 with Tr1C and Tr2C in the presence and absence of Ca^{2+} (25 mM Tris at pH 8, 20°C)*

Ionic strength (mM)	K_d IQ3 (nM)	K_d IQ4 (nM)	Ionic strength (mM)	K_d IQ3 (nM)	K_d IQ4 (nM)
apo-Tr1C			**holo-Tr1C**		
15	88 (15)	405 (95)	30	21 (5.5)	7.7 (2.9)
20	225 (41)	1290 (360)	50	45 (9)	12.3 (3.8)
25	366 (70)	2100 (520)	70	62 (8)	nd
30	559 (67)	2430 (830)	**110**	**120 (13)**	**38.3 (9.5)**
40	1220 (280)	7150 (1920)	150	173 (35)	nd
50	2380 (520)	nd	210	289 (90)	75 (27)
60	3880 (350)	16,500 (4380)	410	555 (149)	nd
110	**~20,000**[a]	~100,000[a]			
apo-Tr2C			**holo-Tr2C**		
20	1.07 (0.28)	1.7 (0.47)	50	2.85 (0.7)	4.7 (1.8)
30	1.65 (0.27)	4.5 (1.2)	75	4.3 (1.6)	nd
40	9.5 (2.3)	21 (6.8)	**110**	**11 (1.5)**	**25 (8.2)**
50	11.2 (2.8)	23 (6.3)	210	18 (2.6)	50 (13.1)
70	28.5 (5.7)	58 (12.3)	310	29 (5.3)	71 (18.3)
110	**82 (18)**	**176 (49)**	410	39 (8.9)	108 (36.5)
150	255 (42)	nd			
220	920 (155)	1650 (470)[b]			
apo-CaM					
110	**21.5 (4.5)**	**33 (8.8)**			
150	59 (6.8)	73 (14)			
210	250 (65)	465 (165)			
310	565 (125)	800 (240)			

[a] These values were estimated by extrapolation from values measured at lower ionic strengths (see text).
[b] A value of 1400 (600) was determined by far-UV CD titration (see text).
Values in parentheses are standard deviations.

interaction of IQ3 (or IQ4) with apo-Tr1C prevents a direct comparison from being made of all complexes under the standard buffer condition of 100 mM KCl. However, a linear extrapolation of the data indicates K_d values of ~20 μM and ~100 μM for the complexes of apo-Tr1C with IQ3 and IQ4, respectively. These may be compared with values of 120 nM and 38 nM for the corresponding complexes with holo-Tr1C. Thus, at an ionic strength approximating normal physiological conditions (typically 100 mM KCl), there is little or no interaction of the peptide with the isolated apo-N domain. In contrast, both IQ3 and IQ4 bind relatively strongly to apo-Tr2C (K_d = 82 nM and 176 nM, respectively) and even more strongly to holo-Tr2C (K_d = 11 nM and 25 nM, respectively). Thus, binding of these peptides to Tr2C is generally significantly stronger than to Tr1C. In all cases the presence of Ca^{2+} causes a significant increase in the affinity of complex formation between either IQ peptide and the individual calmodulin domains, being particularly marked (200- to 2500-fold) for Tr1C, and, in spite of the overall higher affinity, it is still substantial (~10-fold) for Tr2C.

Interaction of IQ3 and IQ4 with calmodulin

The interaction of IQ3 or IQ4 with apo- or holo-CaM was studied by similar methods and over a similar range of solution conditions to determine the contribution of the two domains of the protein to the stoichiometry and affinity of complex formation. The titration of IQ3 with holo-CaM does not show simple 1:1 stoichiometry. At both high and low ionic strength there is an apparent end point at [CaM]/[IQ3] ~ 0.5 (Fig. 5A), indicating that the intact protein can bind two copies of the peptide. To clarify this point, near-UV CD was used as an independent indicator of the interactions of the individual domains of CaM with the Trp-containing region of IQ3. Figure 6A shows a comparison of the near-UV CD difference spectra of the 1:1 complexes of IQ3 with holo-Tr1C and holo-Tr2C with that of a mixture of IQ3 with excess holo-CaM. The latter spectrum clearly resembles that of the 1:1 holo-Tr2C–IQ3 complex. This indicates that IQ3 binds more strongly to the C domain than to the N domain of holo-CaM, as anticipated from the relative affinities of holo-Tr1C and holo-Tr2C for IQ3. In addition, a CD difference titration of IQ3 with holo-CaM was performed, monitoring the CD intensity at 286 nm (Fig. 6B). The signal initially decreases, reaches a minimum at [CaM]/[IQ3] ~ 0.5, and then increases again to become positive at high [CaM]/[IQ3] ratios. This is readily explained in terms of the properties of the complexes of IQ3 with the individual domains (Fig. 6A). The first part of the titration (up to [CaM]/[IQ3] = 0.5) arises because each domain of CaM

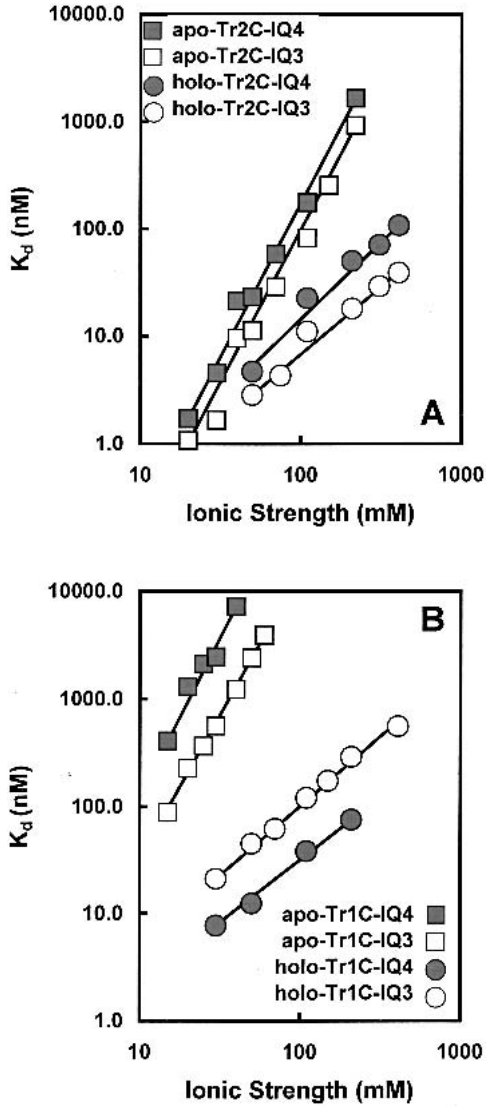

Fig. 4. Ionic strength dependence of the dissociation constants for the interaction of IQ3 and IQ4 with apo- and holo-Tr2C (*A*) and with apo- and holo-Tr1C (*B*). All measurements were made at 20°C in 25 mM Tris (pH 8.0) with 0.2 mM EGTA or 1 mM $CaCl_2$ and KCl as necessary.

binds one IQ3 and the signal is dominated by the more intense negative contribution from the IQ3 bound to the N-terminal domain (cf. holo-Tr1C–IQ3). As the calmodulin concentration is increased further, the two domains effectively compete for the available peptide. The (negative) signal then decreases and becomes positive, eventually resembling the weakly positive CD signal of the holo-Tr2C–IQ3 complex. This follows the pattern of K_ds of 11 and 120 nM for holo-Tr2C–IQ3 and holo-Tr1C–IQ3 complexes, respectively. Thus at high [CaM]/[IQ3] ratios the bulk of the peptide will be bound to the C-terminal domain and the spectrum then resembles that of the holo-Tr2C–IQ3 complex.

This model, in which a peptide can interact with each domain of calmodulin, has been further tested, using the fluorescence and CD titrations of IQ3 with holo-CaM (Figs. 5A and 6B). The optical properties of the bound peptides were assumed to be the same as those of the complexes with holo-Tr1C and holo-Tr2C. The CD data could be adequately described using fixed K_ds of 120 (for the N domain) and 11 nM (for the C domain). Under normal ionic strength conditions (I = 110 mM), the fluorescence curve could be fitted with two emitting species with a relative intensity of 1.26 (as for holo-Tr2C–IQ3/holo-Tr1C–IQ3), and K_ds of 65 ± 25 nM (for the N domain) and 7 ± 2 nM (for the C domain). Given the limitations of the analysis, these values are in good agreement with the K_ds determined for

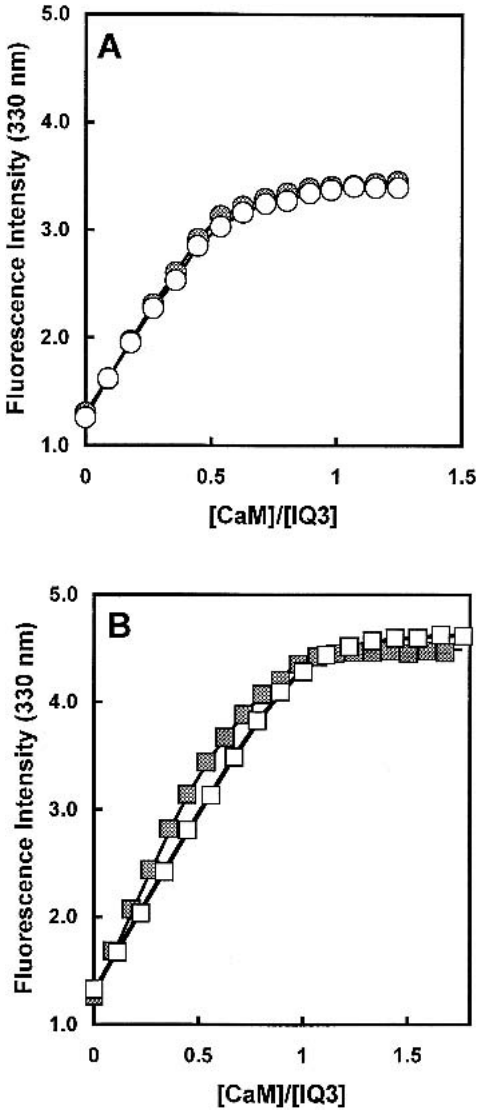

Fig. 5. Fluorescence titrations of IQ3 (2.55 μM) with holo-CaM (*A*) and apo-CaM (*B*). Titrations were performed at 20°C in 25 mM Tris (pH 8.0), 100 mM KCl (open symbols), or 10 mM KCl (closed symbols), with 0.2 mM EGTA or 1 mM $CaCl_2$ as necessary. The solid lines are the computed best fits for the binding of up to two molecules of IQ3 per calmodulin (see text).

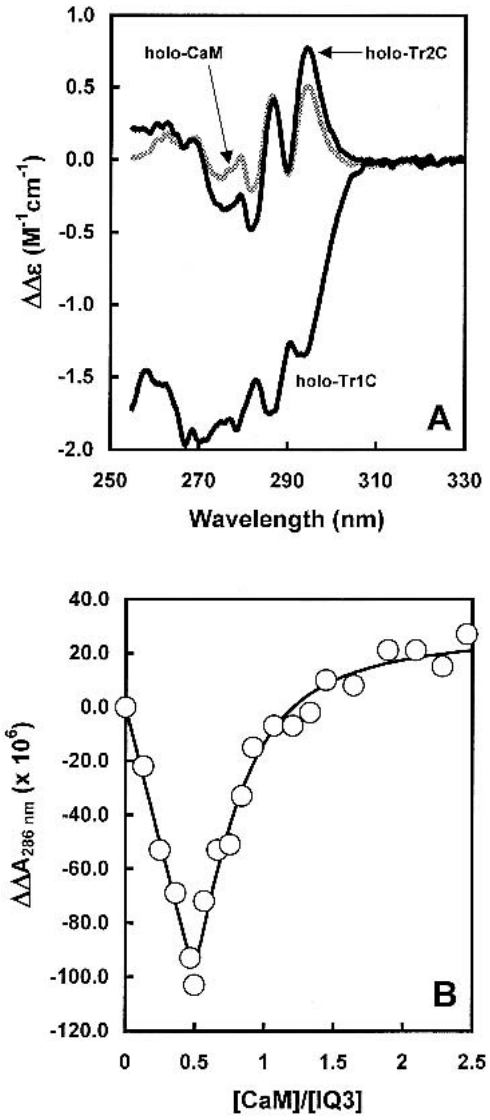

Fig. 6. (*A*) Near-UV CD difference spectra (complex – components) of the complexes of IQ3 with holo-Tr1C, holo-Tr2C, and holo-CaM. The [Protein]/[IQ3] ratio was 1.05 for the fragments and 2.6 for intact calmodulin (see text). The spectra were recorded at 20°C in 25 mM Tris (pH 8.0), 100 mM KCl, 1 mM $CaCl_2$. (*B*) Near-UV CD titration of IQ3 (150 μM) with holo-CaM. The titration was performed at 20°C in 25 mM Tris (pH 8.0), 100 mM KCl, 1 mM $CaCl_2$. The solid line was calculated as described in the text.

the isolated fragments. For the similar titration under low ionic strength conditions (I = 20 mM), the affinity for the holo-C domain was consistently 10 times higher than the affinity for the N domain, but in view of the higher affinities at this ionic strength only the ratio of the affinities is well determined, rather than their absolute values.

Far-UV CD titrations of apo- and holo-CaM with IQ3 and IQ4 are shown in Figure 7. At low ionic strength (Fig. 7A) all four titrations saturate at a [peptide]/[CaM] ratio of ~2, showing that both peptides can form complexes in which each domain of calmodulin contains a bound peptide. The shape of the curves (two essentially linear portions with larger amplitude in the first) indicates that this is a sequential process with the added peptide binding preferentially to the C-terminal domain of the calmodulin. This would again be consistent with the affinities previously determined for interaction of these peptides with the isolated domains. At high ionic strength (Fig. 7B) the interaction of either peptide with holo-CaM is closely similar to that observed at low ionic strength (i.e., a stoichiometry of 2). However, the curves for interaction with apo-CaM are significantly different, and indicate the formation of simple 1:1 complexes. This is consistent with the observation that the isolated

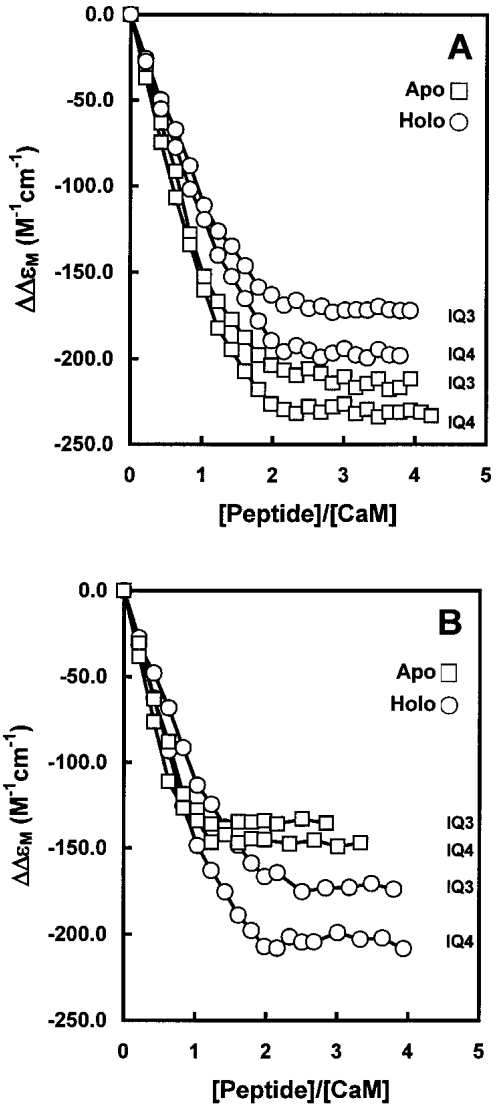

Fig. 7. Far-UV CD titrations (222 nm) of apo- and holo-CaM with IQ3 and IQ4 in the presence of 10 mM KCl (*A*) or 100 mM KCl (*B*). Titrations were performed using 10–12 μM calmodulin at 25°C in 25 mM Tris (pH 8.0) with 0.2 mM EGTA or 1 mM $CaCl_2$ as appropriate.

apo-N domain binds very weakly to IQ3 (and IQ4) at high ionic strength.

The fluorescence titration of IQ3 with apo-CaM (Fig. 5B) at high ionic strength indicates the formation of a simple 1:1 complex. At low ionic strength, the titration is consistent with each domain of CaM binding one molecule of the peptide. The form of the low ionic strength curve is different from that of holo-CaM (Fig. 5A), because the ratio of fluorescence intensities at 330 nm (Tr2C–IQ3/Tr1C–IQ3) is 1.26 in the presence of Ca^{2+}, but 1.78 in the absence. As expected, the data at low ionic strength could be adequately described using fixed K_ds of 225 nM (for the isolated N domain) and 1.07 nM (for the isolated C domain) with two emitting species with a relative intensity of 1.78.

Because both IQ3 and IQ4 form simple 1:1 complexes with apo-CaM at high ionic strength, dissociation constants were determined using direct fluorometric (IQ3) and competition (IQ4) titrations as above. The K_d values for apo-CaM–IQ3 are 21.5 nM (at I = 110 mM), 59 nM (I = 150 mM), 250 nM (I = 210 mM), and 565 nM (I = 310 mM). The K_d values for apo-CaM–IQ4 are 33 nM (at I = 110 mM), 73 nM (I = 150 mM), 465 nM (I = 210 mM), and 800 nM (I = 310 mM). These values may be compared with those for the interaction of the peptides with apo-Tr2C (apo-Tr2C–IQ3, 82 nM and 920 nM; and apo-Tr2C–IQ4, 176 nM and 1650 nM; at I = 110 mM and 220 mM, respectively). This shows that the interactions have a similar sensitivity to ionic strength for both apo-CaM and the apo-Tr2C domain, and that, for both peptides, the interaction with intact apo-CaM is only some four- or fivefold stronger than with the isolated apo-C domain. This further confirms that it is the C-terminal domain of intact calmodulin that interacts with IQ3 under these conditions, with the small increase in affinity resulting from some weak interaction with the apo-N domain.

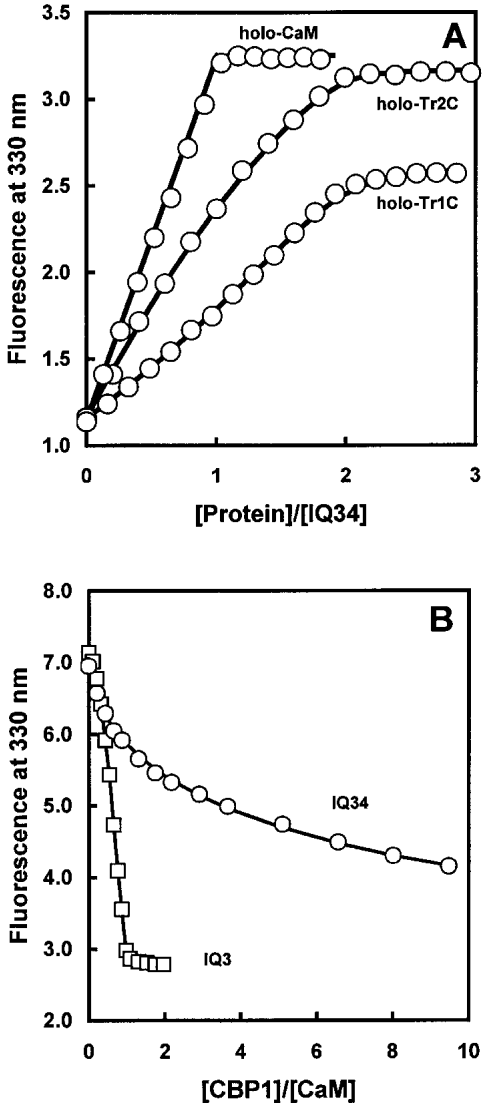

Fig. 8. (*A*) Fluorescence titrations of IQ34 (2.5 μM) with holo-Tr1C, holo-Tr2C, and holo-CaM. The solid lines were calculated as described in the text. (*B*) Fluorescence competition titrations of holo-CaM (5.5 μM) plus 5.8 μM IQ3 or 5.8 μM IQ34 with CBP1. The solid lines are the computed best fits.

Interaction of IQ34 with CaM and the CaM fragments

Because IQ3 and IQ4 are contiguous in the IQ region of myosin V, it is of particular interest to compare the above results with the affinity and Ca^{2+}-sensitivity of the binding of calmodulin and its fragments to the double-length sequence IQ34. It may be noted that IQ34 contains only a single Trp residue in the IQ3 portion. The fluorescence emission spectra of the complexes of IQ34 with calmodulin and the fragments are, as expected, very similar to those of the corresponding complexes with IQ3. Fluorescence titrations of IQ34 with these proteins are shown in Figure 8A. The data for the tryptic fragments are consistent with the binding of two copies of the domain to one IQ34. The titration with holo-Tr2C is convex relative to the abscissa, whereas that with holo-Tr1C is concave. This is consistent with the observed preferences of the domains for the isolated IQ3 and IQ4 peptides: holo-Tr2C binds somewhat more strongly to IQ3 than to IQ4, whereas holo-Tr1C binds somewhat more strongly to IQ4. Furthermore, the computed fits to the fluorescence data show that they can be adequately described using fixed K_d values of 120 (for the N domain) and 11 nM (for the C domain). Thus in binding to IQ34, the higher-affinity interaction for holo-Tr2C is to the Trp-containing, IQ3 portion of the IQ34 sequence, whereas the higher-affinity interaction for holo-Tr1C is to the IQ4 portion of the sequence.

In contrast, the binding of holo-CaM to IQ34 under identical conditions (Fig. 8A) clearly shows the formation of a simple 1:1 complex, consistent with both the constituent N-domain and C-domain binding to the IQ34. The affinity

of the interaction between holo-CaM and IQ34 is clearly high. The K_d has been measured using competition assays with the peptide CBP1 (LKLKKLLKLLKKLLKLG), which also binds to holo-CaM with very high affinity ($K_d \sim 5$ pM; Brown et al. 1997). The results are shown in Figure 8B. A control titration of holo-CaM (5.5 μM) + IQ3 (5.8 μM) with CBP1 shows complex behavior because the initial mixture of IQ3 and holo-CaM contains Ca_4CaM, Ca_4CaM–IQ3, and Ca_4CaM–$(IQ3)_2$ (see above). The titration is initially nonlinear because the IQ3 displaced in the early part of the titration simply forms more Ca_4CaM–$(IQ3)_2$. The important observation is that all the IQ3 is effectively displaced when CBP1 is equimolar with calmodulin, consistent with the fact that CBP1 binds very much more strongly. The titration of holo-CaM (5.5 μM) + IQ34 (5.8 μM) with CBP1 shows very different behavior; IQ34 clearly binds very much more strongly and is only substantially displaced in the presence of a very large molar excess of CBP1. Analysis of this curve yields a K_d for the CaM–IQ34 complex of ~0.6 pM. This value is consistent with each domain binding tightly to an IQ motif, based on the previous measurements of the IQ peptides with the isolated domains. This high affinity also implies that the apparent affinity of calmodulin for Ca^{2+} is significantly enhanced in the presence of the target.

Far-UV CD titrations further confirmed the stoichiometries of 1:1 for the complex of IQ34 with holo-CaM and 2:1 with either of its fragments (Fig. 9A). In addition, these titrations indicate the high α-helicity of the holo-CaM–IQ34 complex. The increase in signal ($\Delta\Delta\varepsilon$) is slightly greater than the mean of the other two plateaus (representing complexes with two domains per IQ34). This indicates that, in the case of the holo-CaM–IQ34 complex, the N domain and the C domain interact with a different portion of the peptide. From the previous data, the most likely orientation would be C domain with the IQ3 portion and N domain with the IQ4 portion. The titration data alone do not exclude the formation of a larger complex in which the proportions of CaM and IQ34 are equimolar, but possibly representing a dimeric (2:2) or higher-order structure. We have therefore examined the complex by equilibrium ultracentrifugation (see Materials and Methods). Nine data sets were globally fitted to a single species model. The best fit to all data sets gave a value of M_r of 21,398 ± 1180 D ($n = 9$), compared with the calculated value of 21,991 D for a 1:1 Ca_4CaM–IQ34 complex. The choice of model was validated by the absence of systematic deviation of the residuals between the fitted curve and all nine data sets. We conclude that the complex is indeed monomeric, involving a single molecule of calmodulin and a single molecule of IQ34 peptide.

In the absence of Ca^{2+}, the fluorescence emission spectra of the complexes of IQ34 with CaM and its fragments are similar, although not identical, to those of the corresponding complexes with IQ3. Fluorescence titrations of IQ34 with

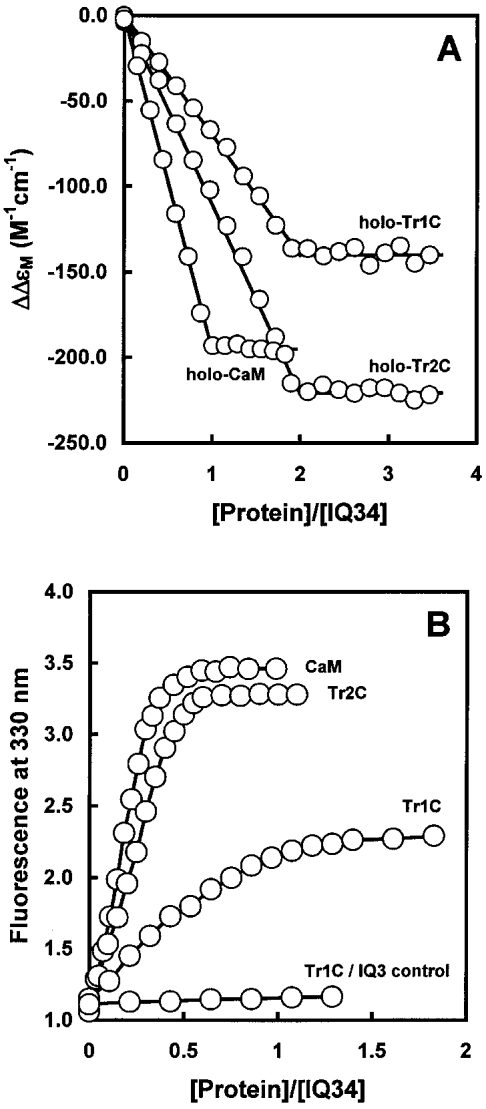

Fig. 9. (*A*) Far-UV CD titrations (222 nm) of IQ34 with holo-Tr1C, holo-Tr2C, and holo-CaM. Titrations were performed using 10–12 μM protein at 25°C in 25 mM Tris (pH 8.0), 100 mM KCl, 1 mM $CaCl_2$. (*B*) Fluorescence titrations of IQ34 (2.3 μM) with apo-Tr1C, apo-Tr2C, and apo-CaM. A control titration of IQ3 (2.3 μM) with apo-CaM is also shown.

the apo-proteins in the presence of 100 mM KCl (Fig. 9B) show several surprising features. The titration with apo-Tr2C appears to show an end point at a [Tr2C]/[IQ34] ratio of close to 0.5, indicating that this fragment is able to bind two copies of IQ34. In the case of apo-Tr1C, the data do not conform well to a simple 1:1 reaction, but the stoichiometry is unclear. In addition, apo-Tr1C appears to bind to IQ34 under ionic strength conditions where it binds only very weakly to either IQ3 or IQ4. The titration of IQ34 with apo-CaM appears to saturate at a [CaM]/[IQ34] ratio of somewhat less than 0.5, indicating that one apo-CaM interacts with multiple IQ34 molecules. Because both the calmodulin and IQ34 are potentially bivalent, the possibility

exists for multimeric complexes, possibly formed by a mixture of specific and nonspecific interactions. The characterization of the complexes of IQ34 with apo-CaM and the fragments in the absence of Ca^{2+} is somewhat limited, because slow aggregation reactions occur even at low concentrations.

Discussion

Calmodulin is well recognized as the ubiquitous cytoplasmic protein that transduces Ca^{2+} signals to activate numerous cellular processes (Chin and Means 2001). However, early work (Cimler et al. 1985; Alexander et al. 1987) identified neuromodulin as a protein with similar affinity for either apo-CaM or Ca_4CaM. At low ionic strength, calmodulin affinity is in fact fivefold to 10-fold higher than in the absence of Ca^{2+}; but at physiological ionic strength, the presence of Ca^{2+} has little effect. Subsequently, a large number of proteins containing the IQ-type calmodulin-binding motif have been identified as able to bind apo-CaM with significant affinity (Bähler and Rhoads 2002). Among these proteins, the unconventional (cytoplasmic) myosins are particularly interesting because (1) they contain multiple IQ-sequences; (2) apo-CaM binds to the functionally important lever-arm region of the proteins; (3) Ca^{2+} inhibits the actin-based motility of several unconventional myosins; and (4) a mechanism has been proposed for this inhibition, in terms of $Ca2^{+}$ causing partial dissociation of calmodulin from the IQ region of myosin I and myosin V (Coluccio and Bretscher 1987; Collins et al. 1990; Swanljung-Collins and Collins 1991; Wolenski et al. 1993; Houdusse et al. 1996; Zhu et al. 1996; Whittaker and Milligan 1997; Homma et al. 2000). This mechanism derives from the properties of neuromodulin, and is based on a general, but (as shown by Bähler et al. 1994) not completely exclusive preference for the IQ motif to bind apo-CaM rather than Ca_4CaM.

This work addresses the central question of the affinity of calmodulin and its domains for sequences in the IQ region of myosin V. Whereas calmodulin appears to be able to act as the principal light chain of mouse myosin V (Trybus et al. 1999; Wang et al. 2000), the light chain binding to the highly homologous IQ1 sequence of chicken myosin V appears to be a specialized (i.e., noncalmodulin, non-Ca^{2+}-sensitive) ELC (De La Cruz et al. 2000). We have therefore concentrated on the central IQ3 and IQ4 sequences of the neck motif of myosin V, which typically acts as the functional target for apo-CaM.

The measurement of the affinity of interaction of the IQ3 and IQ4 peptides with the isolated domains of calmodulin clearly shows that all the interactions are stronger in the presence of excess Ca^{2+}. This result was unexpected in view of the reports that at $[Ca^{2+}] = 1$ mM, at least one calmodulin molecule can be dissociated from the IQ region of either myosin I or V (see above). Furthermore, in the interactions with either IQ3 or IQ4, either in the presence or absence of Ca^{2+}, the C domain, either by itself, or as part of intact calmodulin, binds more strongly than the N domain. In the absence of Ca^{2+}, the N domain is estimated to interact only weakly with either the IQ3 or the IQ4 sequence at physiological ionic strength (~100 mM KCl), and it is found to have ~200-fold lower affinity for a given IQ sequence than the C domain. Time-resolved anisotropy studies of complexes of IQ3 or IQ4 with apo-CaM labeled in either the N or C domain with Alexa-488 show the greater mobility of the N domain (Bayley et al. 2002; P.M. Bayley, S.R. Martin, J.P. Browne, and C.A. Royer, in prep.). In the presence of Ca^{2+}, the N-domain affinity increases markedly (K_d decreases from 20 μM to 100 nM), whereas the C-domain affinity increases only ~10-fold (K_d decreases from 100 nM to 10 nM). The interactions of intact calmodulin with IQ3 and IQ4 are consistent with these values. In the absence of Ca^{2+}, calmodulin binds one molecule of IQ3 (or IQ4), and the affinity is largely accounted for by the C-domain interaction. In the presence of Ca^{2+}, calmodulin can bind two molecules of either IQ3 or IQ4. Hence, both the C domain and the N domain of Ca_4CaM can interact with either peptide.

The interactions of separate domains with the concatenated IQ34 sequence show that in the presence of Ca^{2+}, the N domain interacts somewhat more strongly with the IQ4 portion of IQ34 than does the C domain, whereas the C domain binds more strongly to the IQ3 portion of IQ34, as found for the binding of isolated domains to the separate IQ3 and IQ4 peptide sequences. Consistent with these quantitative results, the binding of calmodulin to the IQ34 peptide in the presence of Ca^{2+} results in a novel 1:1 complex. This stoichiometry is confirmed by (1) the sharp end point of the fluorescence titration; (2) the high affinity of complex formation ($K_d \sim 1$ pM), indicating contributions from both domains; (3) the size of the increase in the far-UV CD signal, indicating increased α-helicity in both IQ3 and IQ4 portions; and (4) the molecular mass by hydrodynamic methods, which confirms that the complex is indeed that of a single molecule of calmodulin with a single IQ34 peptide.

Thus, the observed affinities do not of themselves predict that Ca^{2+} would induce dissociation of calmodulin from IQ3 or IQ4, as might have been expected by analogy with the case of the single IQ sequence containing peptide of neuromodulin (see above). In contrast, the results with the concatenated IQ34 sequence indicate that increased $[Ca^{2+}]$ may cause an individual calmodulin molecule to bind with high affinity, at least to the central motifs of the IQ region of myosin V, to form a specific and stable 1:1 complex. The spectroscopic evidence indicates that both N and C domains can interact with the residues of the IQ motif itself. Also, fluorescence and near-UV CD data indicate similar properties of the Trp residue of the IQ3 sequence in position +3 from the IQ motif, in complexes of Ca_4CaM and IQ3 or

IQ34. Together with the observed affinities of separate holo-N and C domains for IQ34, this evidence strongly indicates the assignment that the C domain interacts with the IQ3 portion, and the N domain with the IQ4 portion of IQ34.

These results with IQ34 also have important structural implications, which may be illustrated with reference to the structure of the scallop regulatory unit (1wdc.pdb; myosin 774–837 plus ELC, RLC). This structure has been taken as a general model for concatenated IQ sequences, and specifically used for modeling the interactions of apo-CaM with the BBM1 sequence (Houdusse et al. 1996, 1aji.pdb). Figure 10A shows the myosin heavy chain as a continuous helix, with a 40° curvature at residues 795–796, and finally a sharp bend at W826. The separation along the helix of the two Gln residues in the two adjacent IQ sequences is ~38–

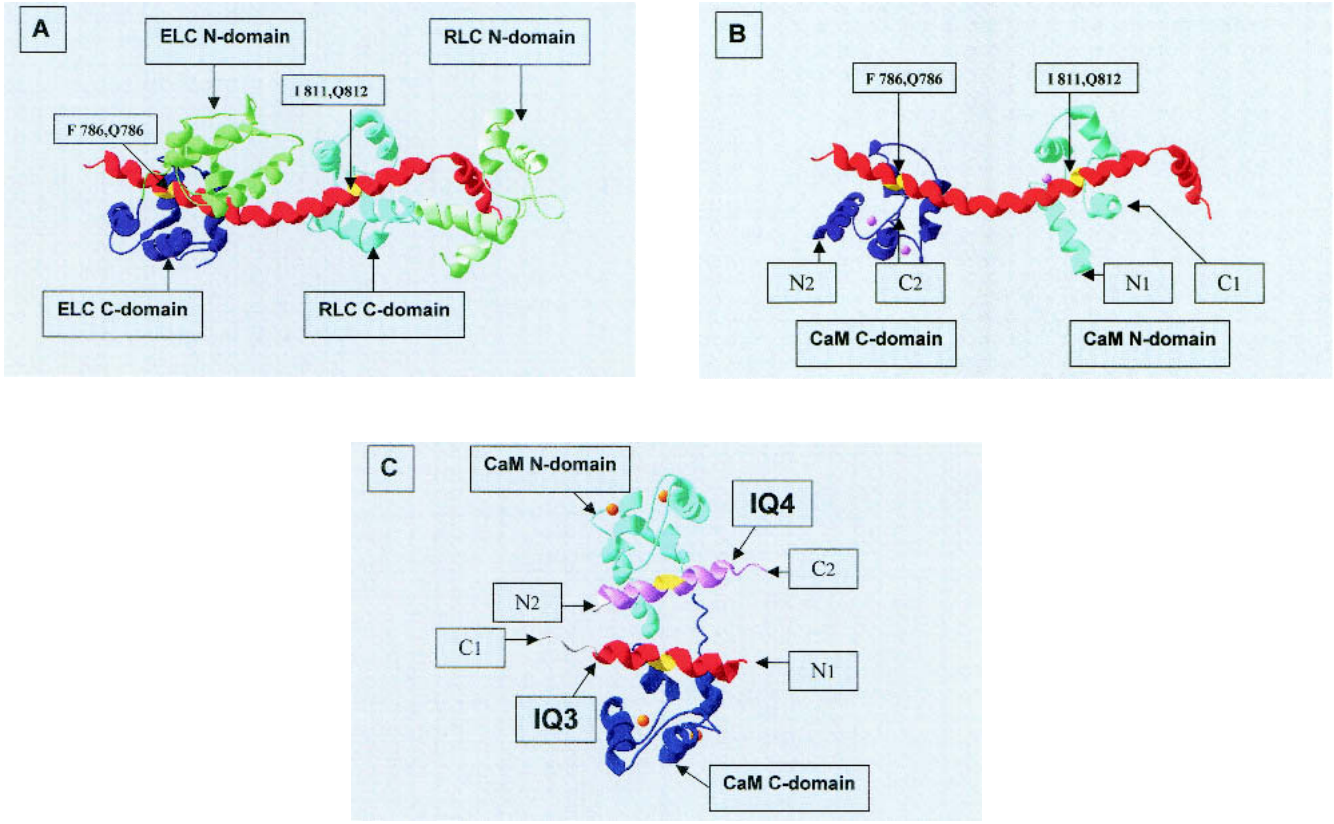

Fig. 10. Derivation of a model for the Ca_4CaM–IQ34 complex based on 1wdc.pdb and 1aji.pdb. (*A*) The structure of the regulatory unit of scallop muscle myosin (1wdc.pdb): myosin heavy chain 774–837 (red). Both of the domains of the essential light chain (ELC, blue, green) and the regulatory light chain (RLC, cyan, pale green) interact with the myosin heavy chain. Their C-terminal domains interact with the IQ sequences based on residues 785, 786 and 881, 882 (yellow). (*B*) Separate superpositions are made of the C domain (blue, residues 76–148) and N domain (cyan, residues 6–76) of Ca_4CaM (4cln.pdb) onto the C domains of ELC and RLC in 1wdc.pdb, respectively. All domain superpositions were made with Swiss Pdb Viewer (Guex and Peitsch 1997) using a least-squares superposition of backbone coordinates of homologous residues in the four helical regions of any pair of domains. In the preferred configuration shown (see text), the connectivity required for calmodulin would be from C1, the C terminus of the N domain (pink, *right*), to N2, the N terminus of the C domain (pale green, *left*). If the alternative connectivity is adopted (i.e., N domain *left* and C domain *right*), the connectivity would be from C2 (pink, *left*) to N1 (pale green, *right*). Neither connectivity appears feasible with calmodulin structure (see text). (*C*) A topological model for the Ca_4CaM–IQ34 complex. Initially, the structure of the C domain of holo-CaM (4cln.pdb) is superimposed onto the C domain of apo-CaM (1 aji.pdb), including the IQ-containing helical peptide of unconventional BBM1 (based on residues 662, 663, yellow). The complex so generated (Ca_2C-domain.BBM1peptide) is then superimposed on both the C domain (blue) and the N domain (cyan) of holo-CaM (4cln.pdb). This calmodulin structure is chosen because it is the maximally extended form of holo-calmodulin with an intact linker sequence. At this point the C and N domains of holo-calmodulin in 4cln configuration carry two (approximately parallel) copies of the IQ peptide. These are now truncated to lengths of 23 and 25 residues, representing the two sequences of myosin V, namely, IQ3 (red) and IQ4 (pink), respectively. The interdomain linker of holo-CaM is in fact partially nonhelical and flexible in solution. This flexibility is simulated by (1) breaking the linker structure at residue 75; (2) rotating one domain (plus its target IQ sequence) by 180° about the linker axis; and (3) tilting one domain (plus target) by ~30° in the plane of the two peptides, to bring the C-terminal residue of IQ3 into close proximity with the N-terminal residue of IQ4. Linking the two termini would produce an antiparallel hairpin structure, involving the two α-helical IQ sequences, bridged by the two calmodulin domains, which are connected by a flexible linker. Sufficient potential latitude exists in the C- and N-terminal residues of IQ3 and IQ4, respectively (gray), to allow for the continuous topology of IQ34. An even more compact structure could be achieved in principle by fully exploiting the flexibility of the calmodulin interdomain linker. The figures were generated using Swiss-PdbViewer V.3.7.

40 Å. It is the C domains of ELC and RLC that interact with the N- and C-terminal IQ motifs, respectively.

In considering whether a single calmodulin molecule could span this distance, we note the need for (1) preservation of the normal helical structure of holo-CaM (as implied by the far-UV CD results), (2) formation in each domain of a hydrophobic site with which the IQ motif is presumed to interact specifically, and (3) the assignment of the calmodulin C-domain interacting with the N-terminal IQ motif of the double IQ sequence. At present there is no high-resolution structure of holo-CaM with an IQ motif. In the model apo-CaM–IQ peptide (1aji.pdb), the calcium-binding loops are remote from the target peptide. We assume that the effect of calcium binding is to cause the change from the semiopen conformation of the apo-C domain to the open conformation of the holo-C domain, so that the orientation of the IQ peptide in the complex with the holo-C domain is the same as that seen in 1wdc and 1aji. The holo-C and holo-N domains have similar open conformations, and their interactions with IQ targets are likely to be closely similar to one another.

Figure 10B shows the results of superimposing the C domain and N domain of holo-CaM on the C domain of the ELC and C domain of the RLC, respectively. This procedure retains the same relative orientation of domain and helical peptide, produces an optimal superposition of the semiopen and open conformations of domains, and allows comparison of the overall topologies. In the preferred assignment of the calmodulin C domain replacing the ELC C domain (Fig. 10B), the distance between the last residue of the N domain and the first residue of the C domain is ~65 Å, that is, far exceeding the potential span of calmodulin. In the reversed assignment, with holo-CaM-N domain and holo-CaM-C domain replacing the C domains of ELC and RLC, respectively, this distance is shorter, approximately 38 Å. Even so, such a distance could only be spanned by the conversion of a significant number of residues from helix D (N domain) and helix E (C domain) of calmodulin into an extended form, for which there is no experimental evidence. We conclude that the double-length IQ sequence of IQ34 cannot exist as a continuous helix in the observed monomeric 1:1 complex with holo-calmodulin.

Figure 10C shows the derivation of an illustrative topological model of the complex of Ca_4CaM–IQ34 that is consistent with the experimental observations. Thus, although the resulting model is not an exact molecular structure, it serves to illustrate the topology required to satisfy the observed set of interactions within reasonable distance constraints. The magnitude of the far-UV CD change in forming the complex is consistent with ~20 residues of IQ34 adopting α-helical structure, with ~10 residues each in the IQ3 and IQ4 portions. This represents ~40% of the total peptide helical sequence shown in Figure 10D, and approximates to the number of residues involved in the interfaces with either domain. Thus there is considerable scope for additional flexibility from the nonhelical portions of the IQ34, especially in the region between the two IQ motifs, and this would allow additional interactions to occur to further consolidate the complex.

The formation of a bridged complex, in which the C and N domains of calmodulin simultaneously interact with the two adjacent IQ motifs, necessarily imposes the steric requirement of a major conformational change in the IQ34 peptide itself. The extended, continuous double-length α-helical structure (seen in 1wdc.pdb) is apparently stabilized by the binding of both domains of the ELC and RLC light chains. The corresponding sequence in IQ34, with fewer domain interactions, presumably lacks this stabilization, providing further argument against it being continuous in the bridged complex of IQ34 with a single holo-CaM. It may be either severely bent or separated in two parts, probably in the central region between the two IQ sequences.

This model predicts that Ca^{2+} can induce a structural change of the regulatory region, which would potentially affect the integrity of the lever arm, and hence motility, of the myosin V. The available evidence indicates that each individual IQ motif in an unconventional myosin interacts with a single light chain, generally apo-CaM. In contrast, the model structure has 1 Ca_4CaM molecule interacting with 2 IQ motifs, and therefore also predicts a Ca^{2+}-dependent change of stoichiometry in the interaction of calmodulin with concatenated IQ sequences. This could explain the observed Ca^{2+}-dependent dissociation of at least one calmodulin molecule from myosin V (and myosin I; Zhu et al. 1998; Homma et al. 2000). This model also provides some indication of possible structural consequences of the calmodulin dissociation. The IQ motifs in a concatenated sequence may, of course, exhibit different individual binding properties with calmodulin, and with different sensitivities to Ca^{2+}. Based on our results of the affinities of IQ3 and IQ4, binding apparently occurs mainly by interaction of the calmodulin C domain, and this may be a relatively general phenomenon. Although the apo-N domain generally makes a weaker energetic contribution, in the presence of Ca^{2+}, its affinity (for IQ3 and IQ4 targets) increases more dramatically than that of the C domain, so that the holo-N-domain affinity becomes more comparable to that of the holo-C-domain affinity (and in fact exceeds it in affinity for the IQ4). In addition, there is an energetic benefit to the affinity of the two domains being linked together in the same calmodulin molecule (Persechini et al. 1994). Thus there is the paradoxical effect that Ca^{2+} causes increased affinity of both calmodulin domains for the IQ motifs, but the formation of the 1:1 bridged complex of Ca_4CaM–IQ34 actually causes the dissociation of one calmodulin molecule. This is because of the markedly increased affinity of the (Ca^{2+}-loaded) N domain, and the change of the double-length IQ helix into a discontinuous, bent or folded conformation.

Because this complex is formed with high affinity, the apparent affinity for Ca^{2+} of calmodulin in the presence of the IQ34 target sequence will be significantly enhanced; however, this effect would be moderated by possible interactions between adjacent apo-CaM molecules in a concatenated IQ system. Whether this novel bridged mode of CaM-target binding is the sole or predominant action of Ca^{2+} on the IQ region of myosin V cannot be resolved until similar experiments have been performed on the neighboring motifs of this region.

Published results for myosin I and V have suggested that inhibition of motility may occur as low as pCa 6, whereas Ca^{2+}-induced dissociation of calmodulin has generally been observed at pCa ~4 or above. Electron microscopy of myosin I at pCa 3 previously resolved a Ca^{2+}-dependent structural change of the myosin, interpreted as a major change of mass apparently caused by the dissociation of calmodulin (Whittaker and Milligan 1997). The proposed bridged mechanism appears to be consistent with this observation. More recently, while the present work was in preparation, Inoue and Ikebe (2001) reported that pCa ~6 also caused dissociation of calmodulin from (3IQ)-myosin-Iβ. Using truncation of individual IQ motifs, it was shown that this occurs from IQ3, whereas the Ca^{2+}-induced increase in the actin-dependent ATPase was assigned to calmodulin bound to the IQ1 sequence. This interesting result is also consistent with the observations that myosin I truncated to contain only IQ1 does not show Ca^{2+}-dependent regulation of the motility, in terms of Ca^{2+} inhibition of motility, and requirement of exogenous calmodulin for its restoration in the absence of Ca^{2+} (Geeves et al. 2000; Perreault-Micale et al. 2000). However, this Ca^{2+}-dependent regulation is retained in constructs of mouse myosin V containing the motor domain plus IQ1 and IQ2 motifs (Trybus et al. 1999; Homma et al. 2000). These results would also be consistent with the role of pairs of IQ motifs providing a Ca^{2+}-sensitive regulation of motility by calmodulin, involving a conformational change in the structure of the lever arm, consistent with the bridged structure described here for Ca_4CaM–IQ34. It will be very interesting to compare the behavior of other double-length IQ motifs from the unconventional myosins.

In summary, we find that Ca^{2+} enhances interactions of calmodulin with these IQ sequences of myosin V. However, calmodulin dissociation may occur from concatenated multiple IQ sequences, owing to the Ca^{2+}-dependent interaction of a single calmodulin binding to two adjacent IQ sequences. This involves a novel mode of interaction of calmodulin in a bridged 1:1 structure, requiring both a conformational change of the regulatory region, and dissociation of at least one of the calmodulin molecules. Such an interaction occurring with full-length myosin V would provide a possible mechanism for Ca^{2+}-dependent regulation of the structure of the full region of multiple IQ sequences, modulating its function as a lever arm in the actin-based motility of unconventional myosins.

Materials and methods

Proteins and peptides

Drosophila CaM was expressed in *Escherichia coli* and purified as described elsewhere (Browne et al. 1997). The tryptic fragments of CaM were prepared as described (Barth et al. 1998). Proteins were made Ca^{2+}-free by incubating with 5–25 mM EGTA and then desalting by passage though two Pharmacia PD10 (G25) columns equilibrated with Chelex-treated buffer (25 mM Tris at pH 8.0). The peptides (IQ3, IQ4, and IQ34) were purchased from the University of Bristol and were end-protected by N-terminal acetylation and C-terminal amidation. Peptide concentrations were determined spectrophotometrically using calculated ε_{278} values of 9475 M^{-1} cm^{-1} (IQ3), 3885 M^{-1} cm^{-1} (IQ4), and 13,360 M^{-1} cm^{-1} (IQ34; Pace et al. 1995). The concentrations of apo-CaM and apo-Tr2C were also determined spectrophotometrically using ε_{279} = 1874 M^{-1} cm^{-1} (Maune et al. 1992). An approximate concentration of apo-Tr1C was determined using a calculated extinction coefficient of 975 M^{-1} cm^{-1}; a more precise value was determined from far-UV CD measurements using a $\Delta\varepsilon_M$ value of 380 M^{-1} cm^{-1}.

Determination of peptide affinities

Dissociation constants for the interaction of the peptides with holo- and apo-CaM were determined at 20°C in 25 mM Tris (pH 8) buffer containing 1 mM $CaCl_2$ or 0.2 mM EDTA as appropriate. The ionic strength was varied by addition of the appropriate amount of KCl. Dissociation constants for IQ3 were determined by direct fluorometric titration at 330 nm using a SPEX FluoroMax fluorimeter with λ_{ex} = 290 nm. Dissociation constants for IQ4 were determined using a fluorescence competition assay in which this nonfluorescent peptide was used to displace IQ3 from its complex with either apo- or holo-CaM. Four independent titrations were performed, and the average value is reported with its standard deviation. The direct fluorometric titrations of the tryptophan-containing peptide (IQ3 = W) with a calmodulin fragment (C) were fit to the following equation:

$$\text{Fluorescence} = F_{(C)}[C] + F_{(W)}[W] + F_{(CW)}[CW]$$

where the F values are the molar fluorescence intensities. A value for the dissociation constant ($K_{d(W)}$) was obtained from a nonlinear least squares fit to this equation with concentrations calculated by solving:

$$[CW]^2 - (K_{d(W)} + C_T + W_T)[CW] + C_T W_T = 0$$

where the subscript T denotes total concentrations. We also included a factor ($X_{(W)}$) in the fitting equation to correct for errors in the peptide concentration (i.e., actual concentration = $W_T X_{(W)}$). Titrations with $X_{(W)} < 1.1$ or with $X_{(W)} < 0.9$ were rejected.

For the displacement assay the optical signal is fit to the following equation:

$$\text{Signal} = F_{(C)}[C] + F_{(W)}[W] + F_{(S)}[S] + F_{(CW)}[CW] + F_{(CS)}[CS]$$

where S is the spectroscopically silent peptide (IQ4).

A value for the dissociation constant ($K_{d(S)}$) was obtained from a nonlinear least squares fit to this equation with concentrations calculated by solving:

$$[C]^3 + (-C_T + K_{d(S)} + K_{d(W)} + W_T + S_T)[C]^2 + (-C_T K_{d(S)} - C_T K_{d(W)} + K_{d(S)} K_{d(W)} + W_T K_{d(S)} + S_T K_{d(W)})[C] - C_T K_{d(S)} K_{d(W)} = 0$$

with $K_{d(W)}$ fixed at the value determined from the direct titration.

Circular dichroism measurements

The CD spectra of CaM and CaM–peptide complexes were recorded on a Jasco J-715 spectropolarimeter at 20°C in 25 mM Tris, 10 or 100 mM KCl (pH 8.0) plus 1 mM $CaCl_2$ or 0.2 mM EDTA as appropriate. Intensities are reported as differential absorption (ΔA) or as the circular dichroism absorption coefficient ($\Delta\varepsilon_M$) calculated using the molar concentration of peptide or protein. Values of $\Delta\varepsilon_{MRW}$ may be calculated as $\Delta\varepsilon_{MRW} = \Delta\varepsilon_M/N$, where N is the appropriate number of peptide bonds.

Equilibrium analytical ultracentrifugation

Ultracentrifugation measurements were made with a Beckman XL-A analytical ultracentrifuge using a 4-position An60Ti rotor. Each cell had a path length of 1.2 cm. Three solutions of the equimolar mixture of calmodulin and IQ34 peptide were used with absorbances (280 nm) of 0.2, 0.4, and 0.6, that is, calmodulin concentrations of 14, 28, and 42 μM. The solutions were allowed to reach equilibrium at speeds of 15,000, 20,000, and 25,000 rpm, and the absorbance relative to buffer was scanned stepwise at each speed. The partial specific volume of the 1:1 complex (at 20°C) was calculated from its amino acid composition to be 0.726 cm^3/g. The solvent density was calculated to be 1.00413 g/cm^3. The nine resultant data sets were fitted to the appropriate equation using Beckman Optima XL-A/XL-I data analysis software.

Acknowledgments

We acknowledge the help of John Eccleston and Amina Mbabaali, NIMR, with the equilibrium analytical ultracentrifugation measurements, and thank Michael Anson, NIMR, for helpful discussions.

The publication costs of this article were defrayed in part by payment of page charges. This article must therefore be hereby marked "advertisement" in accordance with 18 USC section 1734 solely to indicate this fact.

References

Alexander, K.A., Cimler, B.M., Meier, K.E., and Storm, D.R. 1987. Regulation of calmodulin binding to P-57. A neurospecific calmodulin binding protein. *J. Biol. Chem.* **262:** 6108–6113.

Anson, M., Geeves, M.A., Kurzawa, S.E., and Manstein, D.J. 1996. Myosin motors with artificial lever arms. *EMBO J.* **15:** 6069–6074.

Bähler, M. and Rhoads, A.R. 2002. Calmodulin signalling via the IQ motif. *FEBS Letts.* **513:** 107–113.

Bähler, M., Kroschewski, R., Stoffler, H.E., and Behrmann, T. 1994. Rat myr 4 defines a novel subclass of myosin I: identification, distribution, localization, and mapping of calmodulin-binding sites with differential calcium sensitivity. *J. Cell Biol.* **126:** 375–389.

Barth, A., Martin, S.R., and Bayley, P.M. 1998. Specificity and symmetry in the interaction of calmodulin domains with the skeletal muscle myosin light chain kinase target sequence. *J. Biol. Chem.* **273:** 2174–2183.

Bayley, P.M., Findlay, W.A., and Martin, S.R. 1996. Target recognition by calmodulin: Dissecting the kinetics and affinity of interaction using short peptide sequences. *Protein Sci.* **5:** 1215–1228.

Bayley, P.M., Martin, S.R., Browne, J.P., and Royer, C.A. 2002. Time-resolved anisotropy studies of domain-specific interactions of calmodulin with target sequences of myosin V. *Biophys. J.* **82:** 409A.

Berridge, M.A., Lipp, P., and Bootman, M.D. 2001. The versatility and universality of calcium signalling. *Nat. Rev. Mol. Cell. Biol.* **1:** 11–21.

Brown, S.E., Martin, S.R., and Bayley, P.M. 1997. Kinetic control of the dissociation pathway of calmodulin–peptide complexes. *J. Biol. Chem.* **272:** 3389–3397.

Browne, J.P., Strom, M., Martin, S.R., and Bayley, P.M. 1997. The role of β-sheet interactions in domain stability, folding, and target recognition reactions of calmodulin. *Biochemistry* **36:** 9550–9561.

Cheney, R.E. and Mooseker, M.S. 1992. Unconventional myosins. *Curr. Opin. Cell Biol.* **4:** 27–35.

Chin, D. and Means, A.R. 2001. Calmodulin: A prototypical calcium sensor. *Trends Cell Biol.* **10:** 322–328.

Cimler, B.M., Andreasen, T.J., Andreasen, K.I., and Storm, D.R. 1985. P-57 is a neural specific calmodulin-binding protein. *J. Biol. Chem.* **260:** 10784–10788.

Collins, K., Sellers, J.R., and Matsudaira, P. 1990. Calmodulin dissociation regulates brush border mysoin I (110kD-calmodulin) mechanochemical activity in vitro. *J. Cell Biol.* **110:** 1137–1147.

Coluccio, L.M. and Bretscher, A. 1987. Calcium-regulated cooperative binding of the microvillar 110K-calmodulin complex to F-actin: Formation of decorated filaments. *J. Cell Biol.* **105:** 325–333.

Cope, M.J., Whisstock, J., Rayment, I., and Kendrick-Jones, J. 1996. Conservation within the myosin motor domain: Implications for structure and function. *Structure* **4:** 969–987.

Crivici, A. and Ikura, M. 1995. Molecular and structural basis of target recognition by calmodulin. *Ann. Rev. Biophys. Biomol. Struct.* **24:** 85–116.

De La Cruz, E.M., Wells, A.L., Sweeney, H.L., and Ostap, E.M. 2000. Actin and light chain isoform dependence of myosin V kinetics. *Biochemistry* **39:** 14196–14202.

Drum, C.L., Yan, S.-Z., Bard, J., Shen, Y.-Q., Lu, D., Soelaiman, S., Grabarek, Z., Bohm, A., and Tang, W.-J. 2002. Structural basis for the activation of anthrax adenylyl cyclase exotoxin by calmodulin. *Nature* **415:** 396–402.

Erickson, M.G., Alseikhan, B.A., Peterson, B.Z., and Yue, D.T. 2001. Preassociation of calmodulin with voltage-gated Ca^{2+} channels revealed by FRET in single living cells. *Neuron* **31:** 973–985.

Finn, B.E., Evenäs, J., Drakenberg, T., Waltho, J.P., Thulin, E., and Forsén, S. 1995. Calcium-induced structural changes and domain autonomy in calmodulin. *Nat. Struct. Biol.* **2:** 777–783.

Geeves, M.A. 2002. Stretching the lever-arm theory. *Nature* **415:** 129–130.

Geeves, M.A., Perreault-Micale, C., and Coluccio, L.M. 2000. Kinetic analyses of a truncated mammalian myosin I suggest a novel isomerization event preceding nucleotide binding. *J. Biol. Chem.* **275:** 21624–21630.

Guex, N. and Peitsch, M.C. 1997. SWISS-MODEL and the Swiss-PdbViewer: An environment for comparative protein modeling. *Electrophoresis* **18:** 2714–2723.

Homma, K., Saito, J., Ikebe, R., and Ikebe, M. 2000. Ca^{2+}-dependent regulation of the motor activity of myosin V. *J. Biol. Chem.* **275:** 34766–34771.

Houdusse, A. and Cohen, C. 1996. Structure of the regulatory domain of scallop myosin at 2 Å resolution: Implications for regulation. *Structure* **4:** 21–32.

Houdusse, A., Silver, M., and Cohen, C. 1996. A model of Ca^{2+}-free calmodulin binding to unconventional myosins reveals how calmodulin acts as a regulatory switch. *Structure* **4:** 1475–1490.

Houdusse, A., Kalabokis, V.N., Himmel, D., Szent-Györgyi, A.G., and Cohen, C. 1999. Atomic structure of scallop myosin subfragment S1 complexed with MgADP: A novel conformation of the myosin head. *Cell* **97:** 459–470.

Houdusse, A., Gaucher, J.-F., Mui, S., Krementsova, E., Trybus, K.M., and Cohen, C. 2000. Crystal structure of calmodulin bound to the IQ motifs of myosin V. *Biophys. J.* **78:** 272A.

Inoue, A. and Ikebe, M. 2001. Role of the IQ motifs on the regulation of motor activities of myosin 1β. *Mol. Biol. Cell* **12:** 1606.

Kemp, B.E., Pearson, R.B., Guerriero, V.J., Bagchi, I., and Means, A.R. 1987. The calmodulin binding domain of chicken smooth muscle myosin light chain kinase contains a pseudosubstrate sequence. *J. Biol. Chem.* **262:** 2542–2548.

Kuboniwa, H., Tjandra, N., Grzesiek, S., Ren, H., Klee, C.B., and Bax, A. 1995. Solution structure of calcium-free calmodulin. *Nat. Struct. Biol.* **2:** 768–776.

Kurokawa, H., Osawa, M., Kurihara, H., Katayama, N., Tokumitsu, H., Swindells, M.B., Kainosho, M., and Ikura, M. 2001. Target-induced conformational adaptation of calmodulin revealed by the crystal structure of a com-

plex with nematode Ca^{2+}-calmodulin-dependent kinase kinase peptide. *J. Mol. Biol.* **312:** 59–68.

Linse, S., Helmersson, A., and Forsén, S. 1991. Calcium binding to calmodulin and its globular domains. *J. Biol. Chem.* **266:** 8050–8054.

Martin, S.R., Masino, L., and Bayley, P.M. 2000. Enhancement by Mg^{2+} of domain specificity in Ca^{2+}-dependent interactions of calmodulin with target sequences. *Protein Sci.* **9:** 2477–2488.

Maune, J.F., Klee, C.B., and Beckingham, K. 1992. Ca^{2+} binding and conformational change in two series of point mutations to the individual Ca^{2+}-binding sites of calmodulin. *J. Biol. Chem.* **267:** 5286–5295.

Meador, W.E., Means, A.R., and Quiocho, F.A. 1993. Modulation of calmodulin plasticity in molecular recognition on the basis of x-ray structures. *Science* **262:** 1718–1721.

Osawa, M., Tokumitsu, H., Swindells, M.B., Kurihara, H., Orita, M., Shibanuma, T., Furuya, T., and Ikura, M. 1999. A novel target recognition revealed by calmodulin in complex with Ca^{2+}-calmodulin-dependent kinase kinase. *Nat. Struct. Biol.* **6:** 819–824.

Pace, C.N., Vajdos, F., Fee, L., Grimsley, G., and Gray, T. 1995. How to measure and predict the molar absorption coefficient of a protein. *Protein Sci.* **4:** 2411–2423.

Perreault-Micale, C., Shushan, A.D., and Coluccio, L.M. 2000. Truncation of a mammalian myosin I results in loss of Ca^{2+}-sensitive motility. *J. Biol. Chem.* **275:** 21618–21623.

Persechini, A., McMillan, K., and Leakey, P. 1994. Activation of myosin light chain kinase and nitric oxide synthase activities by calmodulin fragments. *J. Biol. Chem.* **269:** 16148–16154.

Rhoads, A.R. and Friedberg, F. 1997. Sequence motifs for calmodulin recognition. *FASEB J.* **11:** 331–340.

Ruff, C., Furch, M., Brenner, B., Manstein, D.J., and Meyerhöfer, E. 2001. Single-molecule tracking of myosins with genetically amplified domains. *Nat. Struct. Biol.* **8:** 226–229.

Schumacher, M.A., Rivard, A.F., Bächinger, H.P., and Adelman, J.P. 2001. Structure of the gating domain of a Ca^{2+}-activated K^+ channel complexed with Ca^{2+}-calmodulin. *Nature* **410:** 1120–1124.

Soderling, T.R. 1999. Putative roles of the Ca^{2+}-CaM-dependent protein kinase (CaM-kinase) cascade. *Trends Biochem. Sci.* **24:** 232–236.

Swanljung-Collins, H. and Collins, J.H. 1991. Ca^{2+} stimulates the Mg^{2+}-APTase activity of brush border myosin I with three or four calmodulin light chains but inhibits with less than two bound. *J. Biol. Chem.* **266:** 1312–1319.

Swindells, M.B. and Ikura, M. 1996. Pre-formation of the semi-open conformation by the apo-calmodulin C-terminal domain and implications for binding IQ-motifs. *Nat. Struct. Biol.* **3:** 501–504.

Trybus, K.M., Krementsova, E., and Freyzon, Y. 1999. Kinetic characterization of a monomeric unconventional myosin V construct. *J. Biol. Chem.* **274:** 27448–27456.

Tsvetkov, P.O., Protasevich, I.I., Gilli, R., Lafitte, D., Lobachov, V.M., Haiech, J., Briand, C., and Makarov, A.A. 1999. Apocalmodulin binds to the myosin light chain kinase calmodulin target site. *J. Biol. Chem.* **274:** 18161–18164.

Uyeda, T.Q., Abramson, P.D., and Spudich, J.A. 1996. The neck region of the myosin motor domain acts as a lever arm to generate movement. *Proc. Natl. Acad. Sci.* **93:** 4459–4464.

Wang, F., Chen, L., Arcucci, O., Harvey, E.V., Bowers, B., Xu, Y., Hammer III, J.A., and Sellers, J.R. 2000. Effect of ADP and ionic strength on the kinetic and motile properties of recombinant mouse myosin V. *J. Biol. Chem.* **275:** 4329–4335.

Whittaker, M. and Milligan, R.A. 1997. Conformational changes due to calcium-induced calmodulin dissociation in brush border myosin I-decorated F-actin revealed by cryoelectron microscopy and image analysis. *J. Mol. Biol.* **269:** 548–557.

Wolenski, J.S., Hayden, S.M., Forscher, P., and Mooseker, M.S. 1993. Calcium-calmodulin and regulation of brush border myosin-I MgATPase and mechanochemistry. *J. Cell Biol.* **122:** 613–621.

Zhang, M., Tanaka, T., and Ikura, M. 1995. Calcium-induced conformational transition revealed by the solution structure of apo calmodulin. *Nat. Struct. Biol.* **2:** 758–767.

Zhu, T., Sata, M., and Ikebe, M. 1996. Functional expression of mammalian myosin Ib: Analysis of its motor activity. *Biochemistry* **35:** 513–522.

Zhu, T., Beckingham, K., and Ikebe, M. 1998. High affinity Ca^{2+} binding sites of calmodulin are critical for the regulation of myosin Ib motor function. *J. Biol. Chem.* **273:** 20481–20486.